



Spatial Variability of Organic Carbon, CaCO_3 and Nutrient Burial Rates Spanning a Mangrove Productivity Gradient in the Coastal Everglades

Joshua L. Breithaupt,^{1,6*}  Joseph M. Smoak,² Christian J. Sanders,³  and Tiffany G. Troxler^{4,5}

¹College of Marine Science, University of South Florida, 140 7th Ave S, St. Petersburg, Florida 33701, USA; ²University of South Florida, Environmental Science, St. Petersburg, Florida 33701, USA; ³National Marine Science Centre, School of Environment, Science and Engineering, Southern Cross University, Coffs Harbour, New South Wales 2540, Australia; ⁴Southeast Environmental Research Center, Florida International University, Miami, Florida 33199, USA; ⁵Department of Biological Sciences, Florida International University, Miami, Florida 33199, USA; ⁶Present address: Present Address: Department of Biology, University of Central Florida, Orlando, Florida 32816, USA

ABSTRACT

Mangrove wetlands are some of the most important locations of organic carbon (OC) sequestration and storage in the world on a per area basis. The high stocks of soil OC are driven by generally high burial rates and efficient preservation of organic material over past millennia of relatively slow and consistent sea level rise. Although the global average rate of OC burial in mangrove wetlands is relatively high, the range in the literature varies by up to two orders of magnitude. The objective of this research was to measure burial rates of OC, CaCO_3 , and nutrients [total nitrogen (TN) and phosphorous (TP)] across a pronounced ecosystem gradient of productivity and salinity in the coastal Everglades of southwestern Florida, USA. Concentra-

tions and burial rates of both CaCO_3 (range 13–1233 $\text{g m}^{-2} \text{y}^{-1}$) and TP (range 0.10–1.59 $\text{g m}^{-2} \text{y}^{-1}$) decreased significantly with distance from the Gulf of Mexico. In contrast, there was less spatial variability in OC (134 ± 12 (1 SE) $\text{g m}^{-2} \text{y}^{-1}$) and TN (6.2 ± 0.4 $\text{g m}^{-2} \text{y}^{-1}$) burial rates. However, significant ($P < 0.001$) regional differences in OC burial rates were observed relative to mangrove primary productivity. Over a centennial timescale, downstream sites buried 14% of annual net primary production, midstream sites buried 22%, and upstream sites preserved less than 10%.

Key words: organic carbon burial; nitrogen; phosphorous; carbonate burial; mangroves; Everglades.

Received 19 March 2018; accepted 11 September 2018;
published online 5 October 2018

Electronic supplementary material: The online version of this article (<https://doi.org/10.1007/s10021-018-0306-5>) contains supplementary material, which is available to authorized users.

Authors' contributions All authors contributed to study design, conducting research and writing the paper. JLB conducted data analysis.

*Corresponding author; e-mail: Joshua.Breithaupt@UCF.edu

INTRODUCTION¹

Mangrove wetlands are some of the most important locations of organic carbon (OC) sequestration and storage in the world on a per area basis (Donato and others 2011; Mcleod and others 2011). This is due in large part to high stocks of soil OC produced by burial rates that are on average higher than other terrestrial ecosystems (Breithaupt and others 2012; Chmura and others 2003; McLeod and others 2011). Although the global average OC burial rate is relatively high, rates recorded in the literature vary substantially, from a low of $21 \text{ g m}^{-2} \text{ y}^{-1}$ in scrub mangroves of Naples Bay, FL (Marchio and others 2016) to high rates of 1020 and $1023 \text{ g m}^{-2} \text{ y}^{-1}$ in the Jiulongjiang Estuary, China, and Cubatão, Brazil, respectively (Alongi and others 2005; Sanders and others 2014). This wide variability exists in part because of the extensive differences in mangrove forest structure that are driven by eco-geomorphological factors including tidal range, riverine influence, temperature, rainfall and evapotranspiration (Rovai and others 2016; Twilley and Rivera-Monroy 2009). Although these ecosystems are understood to have generally high soil OC stocks and burial rates globally, the extent of the coupling between OC stocks and burial rates in mangrove vegetation and soils is unclear at regional spatial scales. For example, the two highest OC burial rates noted above occurred in estuaries that have been extensively modified by anthropogenic activities; it has been suggested that these high rates are due to a substantial contribution of non-mangrove OC (Sanders and others 2014). Therefore, more recent rates that have been influenced by anthropogenic activities may not be indicative of longer-term processes that have contributed to overall present-day stocks. Global comparisons indicate that approximately 10–15% of net annual mangrove production is buried over a centennial timescale (Bouillon and others 2008; Breithaupt and others 2012). For locations where site-specific C budgets have been conducted, estimates range from burial as 4% of gross primary production in Belize (Lovelock and others 2015), 16–27% of net primary production in Malaysia (Alongi and others 2004), 7–30% in China (Alongi and others 2005), 4–12% in Thailand (Alongi and others 2002) or 6–42% in the Herbert River estuary in Australia (Brunskill and

others 2002). The variability of soil carbon retention has been attributed to climate, topography, mineralogy, tidal conditions, and various biotic variables including plant species traits and the effects of species mixing (Amundson 2001; Breithaupt and others 2012; Chmura and others 2003; Davidson and Janssens 2006; De Deyn and others 2008; Lang'at and others 2013).

Mangrove wetlands in Everglades National Park (ENP) represent an economically and ecologically important coastal margin in southwest Florida. Mangroves in ENP occupy 144,447 ha (Simard and others 2006) of protected land that has been estimated to store 321 Mg of organic carbon ha^{-1} in the biomass and soils (Jerath and others 2016). The total value of this stored C was estimated at \$2–\$3.4 billion USD, with values ranging from \$13,859 to \$23,728 ha^{-1} , based on an assessment of the North American socioeconomic context as well as the protected status of these mangroves (Jerath and others 2016). Despite their value and protected status, these wetlands are vulnerable to a number of significant pressures. Since the beginning of the twentieth century, these mangroves have been subjected to extensive anthropogenic alteration of south Florida hydrology (McVoy and others 2011), a steady rate of regional sea level rise (Maul and Martin 1993) that is potentially accelerating (Haigh and others 2014; Park and Sweet 2015; Wdowinski and others 2016), and numerous tropical storms and hurricanes (Smith and others 1994, 2009). There are growing concerns about the stability of historically sequestered carbon in mangroves both regionally and globally due to a number of these pressures, and it is therefore important to understand the rates at which OC has accumulated across a spatially variable landscape like the coastal Everglades.

Mangroves in the southwest coast of the Everglades are estuarine in terms of hydrology, salinity, and chemistry, and the relatively minor percentage of allochthonous sediment delivery is tidally dominated. Phosphorous (P), is the primary limiting nutrient in this ecosystem (Boyer 2006; Childers and others 2006). During large storms, phosphorous can be supplied to the mangroves of the Everglades when CaCO_3 mud is resuspended in Florida Bay and the Gulf of Mexico and deposited by storm surge (Castañeda-Moya and others 2010; Smith and others 2009; Whelan and others 2009). Groundwater discharge has also been identified as a subterranean source of P in the coastal Everglades (Price and others 2006). As a result, the structure and composition of mangrove wetlands in this region are highly spatially variable (Castañeda-Moya

¹ Non-standard Abbreviations: CNPP: net primary productivity of organic carbon ($\text{g OC m}^{-2} \text{ y}^{-1}$), DBH: diameter at breast height (cm), GOM: Gulf of Mexico, RespC: respired carbon ($\text{g OC m}^{-2} \text{ y}^{-1}$).

and others 2013; Chen and Twilley 1999a). Much of the research conducted in past decades, continuing to the present, has sought to identify how geophysical conditions (including soil characteristics) influence the structure and productivity of mangrove forests (Thom 1982; Boto and Wellington 1984; Twilley 1995; Chen and Twilley 1999a; Rovai and others 2016). Questions remain about the extent to which variability in aboveground forest structure and productivity indicates similar variability of burial rates of soil constituents like OC and CaCO_3 in peat-forming environments like the Everglades. The mangrove nutrient model (Chen and Twilley 1999b; Twilley and Rivera-Monroy 2009) indicates that rates of mangrove production, decomposition and export, combined with addition of marine sediment from the Gulf of Mexico (GOM), explain the estuarine gradient in soil characteristics such as organic matter and nutrient concentrations with depth.

One-hundred-year average OC burial rates have been measured previously (Breithaupt and others 2014) in six cores within a 200-m footprint at a site on the Shark River where mangroves represent the highest standing aboveground biomass, tree height, and productivity in the Everglades (Simard and others 2006; Castañeda-Moya and others 2013). Soil at that site consists of 5.5 m of peat above bedrock (Whelan and others 2005) that has been accreting for the past 5250 years, with mangrove-specific peat accretion beginning 3800 years ago (Yao and others 2015). Breithaupt and others (2014) reported a 100-year mean rate of 123 ± 19 (SD) $\text{g OC m}^{-2} \text{ y}^{-1}$ for six cores. This value is significantly lower than global expectations suggest based on a geometric mean rate of $163 (+40, -31; 95\% \text{ CI}) \text{ g m}^{-2} \text{ y}^{-1}$ derived from the literature (Breithaupt and others 2012) and raises the question of whether the mean rate of $123 \text{ g m}^{-2} \text{ y}^{-1}$ is representative of the broader coastal Everglades region.

The main objective of this study was to examine the spatial variability of 100-year burial rates of OC, CaCO_3 , and nutrients [total nitrogen (TN) & TP] across an estuarine gradient where productivity decreases in the landward direction from the coast. Based on the significant variability in ecosystem-scale aboveground vegetation characteristics (Simard and others 2006; Castañeda-Moya and others 2013; Breithaupt and others 2014), we hypothesized a positive correlation between aboveground vegetation characteristics (that is, biomass, density, complexity index) and OC, TN and TP burial rates. Additionally, based on previous research that has identified a significant decrease in TP and storm-

derived mineral (CaCO_3) sediments as a function of distance from the GOM, we hypothesized that TN/TP would decrease in the upstream, organic sites. For a subset of sites, we tested whether OC burial rates explained variation in soil CO_2 efflux using published data.

METHODS

Study Area

The saline coastal Everglades ecosystem is dominated by mangrove vegetation with peat soils ranging from 1 to 5.5 m thick that overlie carbonate bedrock (Scholl 1964; Whelan and others 2005; Yao and others 2015). Freshwater from upstream Everglades marshes drains to the southwest coast via Shark River Slough and to the southeast via Taylor Slough. It has been estimated that the volume of freshwater reaching these mangroves has been reduced by up to 59% by Everglades drainage and impoundments during the twentieth century (Smith and others 1989). Under present-day conditions, the outflow through Shark Slough is ten-fold higher than that through Taylor Slough (Smith and others 1989). Discharge is a combined result of surface and groundwater flow, precipitation, weather events that influence circulation and semi-diurnal tides. As water from Shark Slough approaches the coast, it is further subdivided into five major outlets from north to south (along with their relative percentage of total drainage): Lostmans Creek (20%), Broad River (26%), Harney River (23%), Shark River (27%), and North River (4%) (1998–2000 estimate; Levesque 2004). River surface water salinities (PSU) at the time soil cores were collected for this project (March 13–14, 2013) ranged from 0.67 to 31.41 on Shark River (sites WSC-1 and WSC-6, respectively), 14.58–28.7 on Harney River (sites WSC-7 and WSC-10, respectively), and 19.69–15.69 on Broad River (sites WSC-11 and WSC-13, respectively). Long-term (1996–2012) averages (± 1 SD) of surface water salinity at USGS stations were 5.7 ± 6.2 at WSC-2, 15.2 ± 9.0 at WSC-8, and 26.0 ± 5.8 at WSC-6 (http://sofia.usgs.gov/exchange/sfl_hydro_data/index.html; Anderson and others 2014). Sites where the soil cores were collected have previously been classified according to their mean loss-on-ignition (LOI) values as Organic ($> 70\%$), Intermediate ($40\text{--}70\%$), and Mineral ($< 40\%$) after a 1-way ANOVA and post hoc Tukey comparisons showed these classes to be significantly different from each other ($F_{(2,461)} = 1793.27$, $P = 0.000$). In general, organic sites were those located farthest upstream

(≥ 13 km from GOM) and mineral sites were farthest downstream (≤ 8 km from GOM) (Table 1). We combined existing published data with new soil, vegetation and OC and nutrient burial rates for riverine mangroves along the Shark, Harney, and Broad Rivers in southwestern Everglades National Park. Riverine transect lengths were 25, 14, and 11 km, respectively (Figure 1; Table 1). Sites WSC-2, 4, 5, and 8 are co-located with stations of the United States Geological Survey (USGS), and Florida Coastal Everglades Long-Term Ecological Research (FCElTER) program, allowing comparisons with long-term ecosystem data. We utilized published data from measurements from the FCElTER for aboveground vegetation characteristics, total (above- and belowground) net primary production (NPP) (Castañeda-Moya and others 2013) and soil respiration (Troxler and others 2015). The OC portion of NPP was assumed to be 44% of the total (Bouillon and others 2008) and is referred to as CNPP hereafter. The carbon portion of soil CO₂ effluxes was scaled to annual rates by multiplying its molar fraction (27.29%) by the fluxes reported by Troxler and others (2015) ($\mu\text{mol m}^{-2} \text{s}^{-1}$) and by the number of seconds in a year, hereafter referred to as Resp_C.

Mangrove Aboveground Vegetation Characterization

Aboveground vegetation was characterized for sites WSC-7–10, 11, and 13 on the Harney and Broad Rivers in October 2015, using 20 × 20 m plots corresponding to soil core locations (Sect. 2.3). We measured stem diameter at breast height (DBH) and stem density for each tree greater than 2.5 cm DBH. From these data, we estimated total basal area ($\text{m}^2 \text{ha}^{-1}$), total dry aboveground biomass (Mg ha^{-1}), stem density (stems ha^{-1}), and site complexity index. Biomass was estimated using allometric equations developed in the Everglades specific to *Rhizophora mangle*, *Avicennia germinans*, and *Laguncularia racemosa* (Smith and Whelan 2006), as well as *Conocarpus erectus* (Abohassan and others 2010). The Holdridge Complexity Index for each site was calculated by multiplying total basal area by stem density by canopy height and by the number of different species present (Holdridge and others 1971; Castañeda-Moya and others 2013). Tree height was estimated using an inclinometer based on measured distance from each trunk. Characteristics for the Shark River sites (WSC-2, 4, and 5) were previously collected by Castañeda-Moya and others (2013) using data collected from 2002–2004.

Soil Characterization and Dating

Soil cores were collected from 13 sites in southwestern Everglades National Park (Figure 1). Six soil cores were collected from site WSC-5 in 2010 using a Russian split barrel corer (5 cm diameter × 50 cm length; Breithaupt and others 2014) and in 2013 single cores were collected from each of the remaining sites using PVC push cores (10 cm diameter × 50 cm length) (Breithaupt and others 2017). Cores were extruded and cut in 2-cm depth intervals over the 0–10 cm depth, and in 1-cm depth intervals until the 40-cm depth. Exceptions were the 6 cores at site WSC-5 and the single core at WSC-10 which were sectioned in 1-cm intervals over the entire core length. Subsamples were collected from sectioned core intervals, then dried at 105° C for measurements of dry bulk density (DBD) (dry mass divided by subsample wet volume), then subsequently combusted for three hours at 550 °C for loss-on-ignition (LOI) measurements of soil organic matter content (Breithaupt and others 2017).

Soil concentrations of OC, TN, and TP were measured for sectioned intervals extending to approximately the 100-year old depth, which ranged from 18 to 38 cm (Breithaupt and others 2017). Samples were acidified to remove carbonate material prior to OC measurements. Nitrogen measurements were conducted on non-acidified material. Analyses were done using a PDZ Europa ANCA-GL (Automated Nitrogen Carbon Analyzer-Gas Solids Liquids) elemental analyzer. The analytical precision of duplicate analyses of standards was 0.28% for C and 0.02% for N. The analysis of TP was conducted on bulk soil using a Perkin Elmer ELAN DRCE ICPMS (Dynamic Reaction Cell-equipped Inductively Coupled Plasma Mass Spectrometer); the Laboratory Control Sample (LCS) was AGAL 12, which was digested and analyzed as part of each batch (Sanders and others 2014).

In addition to the LOI measurement for organic matter, the CaCO₃ content was calculated via a secondary burn in a muffle furnace at 990 °C for 1 additional hour (Dean 1974). By multiplying the mass lost in the second burn (assumed to be CO₂) by 2.27, the total CaCO₃ content of the soils was estimated; $(2.27 \times 44 \text{ (CO}_2 \text{ formula weight)}) = 100 \text{ (CaCO}_3 \text{ formula weight)}$ (Dean 1974). Values would be slightly different if soil concentrations of elemental carbonate compositions were known, including magnesium calcite, siderite, and dolomite.

All soil cores were dated using ²¹⁰Pb and the Constant-Rate of Supply model (Appleby 2001);

Table 1. Mean (\pm 1 SE) Soil Content of Organic Carbon (TOC), Calcium Carbonate (CaCO_3), Total Phosphorous (TP), and Nutrient Ratios by Site and Site Classification

River	Site classification	Site	Distance from GOM (km)	<i>n</i>	TOC (%)	CaCO_3 (%)	TN (%)	TP (mg cm^{-3})	Molar OC/TN	Molar TN/TP
Shark	Organic	WSC-1	25	21	42.5 (0.17)	6.9 (0.30)	2.3 (0.09)	0.08 (0.004)	22.3 (0.83)	96.0 (3.50)
	Organic	WSC-2 ^a	18	13	42.4 (0.22)	6.9 (0.29)	2.1 (0.06)	0.06 (0.003)	23.4 (0.49)	85.8 (2.08)
	Organic	WSC-3	13	16	39.1 (0.42)	5.8 (0.68)	1.7 (0.03)	0.07 (0.004)	26.7 (0.34)	80.7 (2.62)
	Intermediate	WSC-4 ^b	8	31	29.3 (0.27)	20.6 (0.74)	1.5 (0.06)	0.15 (0.003)	22.7 (0.59)	40.3 (2.0)
	Intermediate	WSC-5 ^{c*}	4	30	24.2 (1.43)	n/a	1.3 (0.03)	0.21 (0.005)	21.3 (0.57)	27.0 (0.65)
	Mineral	WSC-6	2	18	15.2 (0.75)	22.3 (1.76)	0.9 (0.04)	0.38 (0.015)	19.0 (0.82)	17.0 (0.29)
Harney	Organic	WSC-7	14	15	37.1 (0.15)	12.2 (0.51)	1.9 (0.04)	0.11 (0.009)	22.7 (0.29)	57.4 (3.33)
	Intermediate	WSC-8 ^d	9	23	29.8 (0.24)	15.5 (0.80)	1.4 (0.03)	0.18 (0.006)	24.5 (0.37)	34.6 (0.63)
	Intermediate	WSC-9	5	30	22.6 (0.52)	23.7 (1.47)	1.3 (0.04)	0.20 (0.006)	20.6 (0.39)	28.9 (0.91)
	Mineral	WSC-10	2	33	10.3 (0.17)	41.8 (2.91)	0.4 (0.02)	0.50 (0.030)	34.7 (1.42)	10.2 (0.41)
	Intermediate	WSC-11	11	26	32.6 (0.46)	12.4 (0.32)	1.5 (0.01)	0.15 (0.007)	24.9 (0.34)	41.8 (1.54)
Broad	Mineral	WSC-12	8	21	16.0 (0.41)	14.4 (2.15)	0.9 (0.04)	0.39 (0.019)	21.8 (0.74)	16.5 (0.54)
	Mineral	WSC-13	2	24	10.1 (0.16)	58.8 (0.85)	0.3 (0.01)	0.47 (0.016)	47.6 (2.60)	10.5 (0.44)
	Organic				40.4 (0.4) A	9.9 (0.5) A	2.0 (0.04) A	0.08 (0.003) A	23.7 (0.53) A	81.3 (3.21) A
	Intermediate				27.4 (0.7) B	19.4 (1.0) B	1.4 (0.02) B	0.18 (0.003) B	22.7 (0.41) A	34.4 (1.34) B
	Mineral				12.4 (0.3) C	41.2 (2.8) C	0.6 (0.03) C	0.44 (0.013) C	32.2 (1.39) B	12.9 (0.57) C

Sample number (*n*) is the number of measured soil intervals. Different capital letters after mean values of site classifications indicate significant difference ($P < 0.05$). Sites that are co-located with sites of the United States Geological Survey (USGS) and Florida Coastal Everglades Long-Term Ecological Research program (FCElTER).

Site co-locations: ^aUSGS SH2 & FCElTER SRS-4, ^bFCElTER SRS-5, ^cUSGS SH3 and FCElTER SRS-6, ^dUSGS SH4.

*Data are from Breithaupt and others (2014).

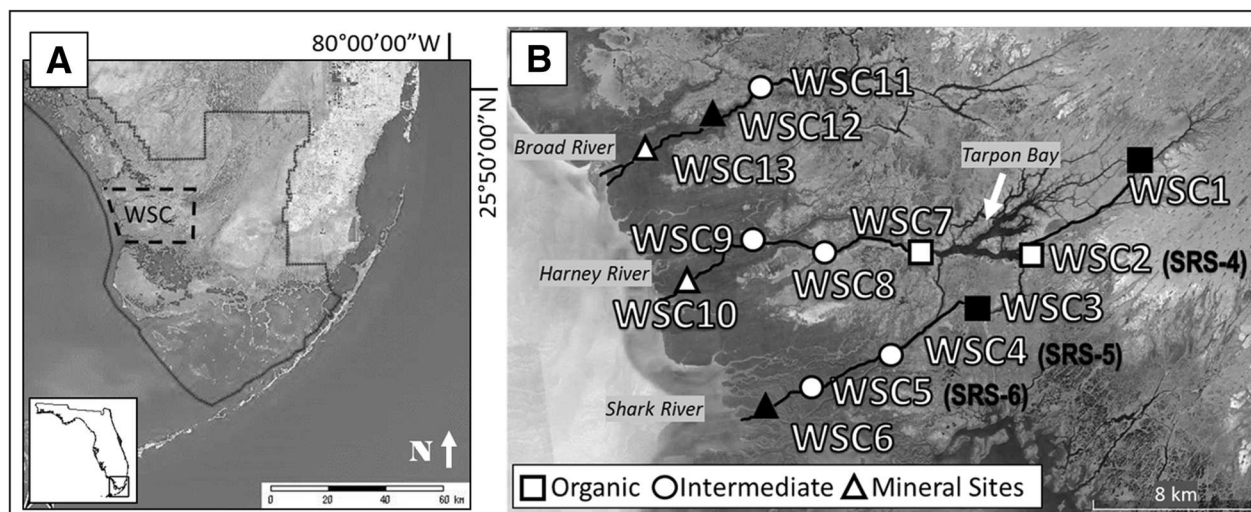


Figure 1. **A** Everglades National Park in southwest FL, USA and **B** WSC primary research core locations on the Shark, Harney, and Broad Rivers. Different shapes in panel (**B**) indicate different soil classes; open (white) shapes indicate sites where vegetation data was collected or available from the literature. Map A created using “Florida Coastal Everglades LTER Mapserver project” <http://fcelter.fiu.edu/gis/everglades-map/>.

this model was utilized to account for variable sedimentation rates observed in this environment (Smoak and others 2013) and provides dates for each core interval containing activities of excess ^{210}Pb . Full methods and results of the dating for these cores, including depth profiles of excess ^{210}Pb activities and accretion rates (mm y^{-1}), are provided in Breithaupt and others (2017), including the Supplementary data. Soil mass accumulation rates were calculated by dividing the total mass (g) for a given unit area (cm^2 or m^2) by the age at depth (y). Burial rates of individual constituents (that is, OC, TN, TP and CaCO_3) were calculated by multiplying the concentration (%) of each by the mass accumulation rate. For this paper, a flux is synonymous with burial rate, where positive values indicate addition to the soil and negative values indicate loss. Uncertainties for soil accumulation rates were calculated by propagating gamma counting uncertainties for core interval dates and soil mass accumulation rates (Binford 1990).

Statistical Analyses

All statistical analyses, including regression fitting, were conducted using Minitab 17. Differences in soil concentrations (TOC%, $\text{CaCO}_3\%$, OC/TN, and TN/TP) or fluxes between the organic, intermediate, and mineral soil classes were tested using Welch’s 1-way ANOVA with post hoc Games-Howell pairwise comparisons. Welch’s ANOVA was used because the assumption of homogeneity of variance was not met. The following transforma-

tions were used when data were found to be non-normally distributed: for timescale comparisons of mean rates by soil class, OC and TN values were raised to the power of -3 . Reported uncertainties represent 1 standard error unless stated otherwise.

RESULTS

Aboveground Vegetation Characteristics

Total aboveground biomass at the thirteen sites ranged from 95.0 (WSC-4/SRS-5) to 162.2 (WSC-5/SRS-6) Mg ha^{-1} (Figure 2A). Basal area ($\text{m}^2 \text{ha}^{-1}$) was lowest at WSC-4/SRS-5 (22.3) and highest at WSC-5/SRS-6 (40.9) (Figure 2B). Stem density (stems ha^{-1}) was lowest at WSC-9 on the Harney River (1500) and highest at site WSC-11 (9675) on the Broad River (Figure 2C). Site WSC-2/SRS-4, an organic site on the Shark River, had a similarly high stem density of 7746 stems ha^{-1} . Site WSC-9 had the lowest site complexity index score (11.7) and site WSC-11 had the highest (108.9) (Figure 2D). Of the four aboveground vegetation parameters that were measured, only stem density was positively correlated with distance from the GOM ($r = 0.72$, $P < 0.05$). There were no significant correlations with any of the measured soil fluxes or nutrient ratios across the region. Additionally, no significant difference was detected between organic, intermediate, and mineral site classifications for any of the four characteristics ($P > 0.05$) (Figure S1), although the statistical power of these comparisons was lim-

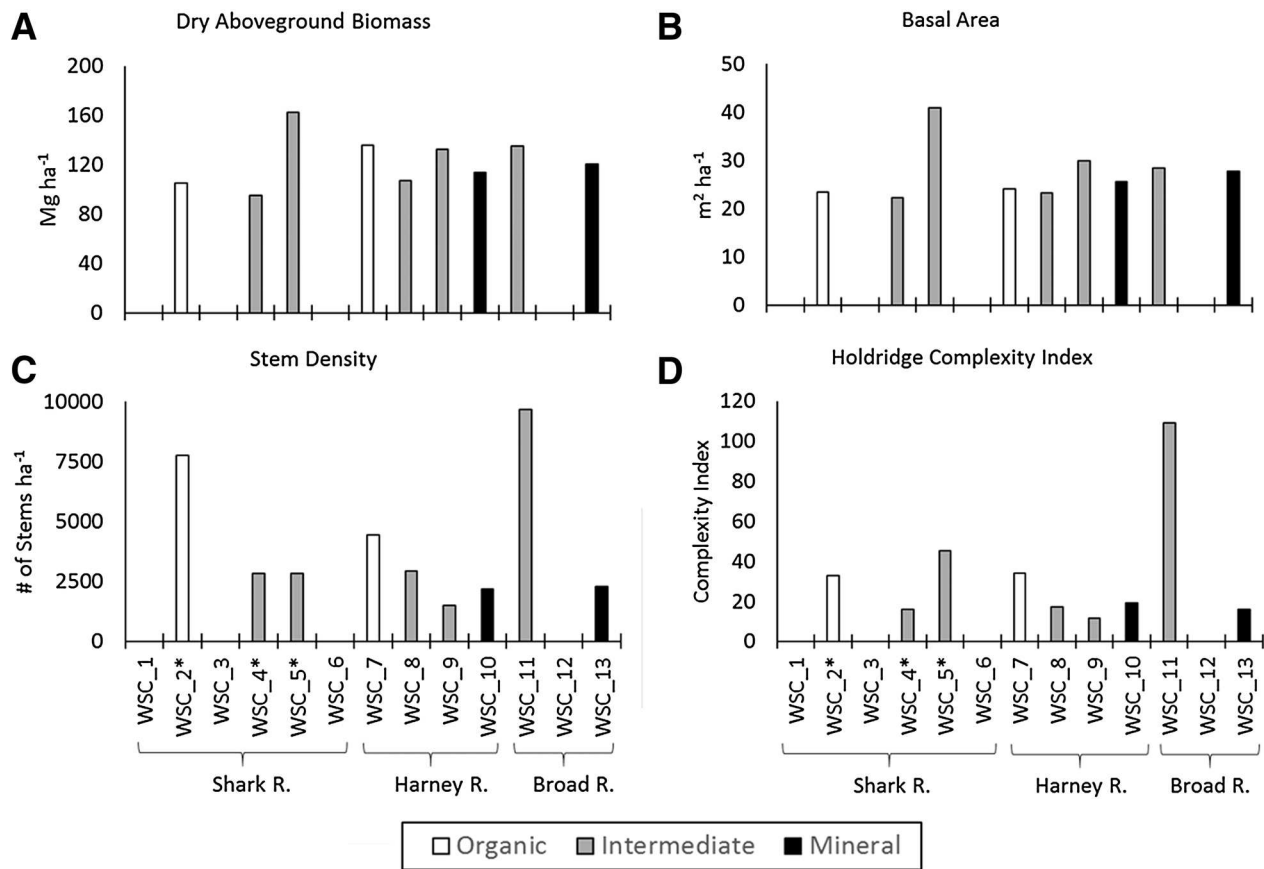


Figure 2. Aboveground biomass characteristics by site for each river and soil class: **A** Dry aboveground biomass, **B** basal area, **C** stem density, and **D** site complexity. Asterisks (WSC-2, 4, and 5) indicate data collected from 2002 to 2004 by Castañeda-Moya and others (2013).

ited because of the small sample size ($n = 2$) for organic and mineral sites.

Soil Concentrations of OC, CaCO_3 , TN, and TP

The highest soil OC concentrations (39–42%) occurred in the upper Shark River sites approximately 13 km or more from the GOM, and the lowest concentrations were found at the river mouths (WSC-13: 10.1%, WSC-10: 10.3%, and WSC-6: 15.2%). In contrast, concentrations of CaCO_3 were highest at the river mouths (WSC-13: 58.8%, WSC-10: 41.8%, and WSC-6: 22.3%) and lowest at sites on the upper Shark River (WSC-1 and 2: 6.9%). When compared by site class, the mean soil OC content decreased significantly ($P < 0.05$) from organic ($40.4 \pm 0.4\%$ of total dry mass) to intermediate ($27.4 \pm 0.7\%$) to mineral sites ($9.3 \pm 0.8\%$) (Table 1). Average concentrations of CaCO_3 increased from organic ($9.9 \pm 0.5\%$) to intermediate ($19.4 \pm 1.0\%$) to mineral ($41.2 \pm 2.8\%$) site classifications.

Spatial patterns of TN concentrations were similar to OC concentrations across sites within the region ($r = 0.61$, $P < 0.05$; Tables 1, 2). Lowest TN concentrations occurred at the river mouths (WSC-13 and WSC-10, 0.3 and 0.4%, respectively), and the highest concentration occurred at site WSC-1 furthest up the Shark River (2.3%). When compared by soil class, TN% increased significantly from mineral ($0.6 \pm 0.03\%$) to intermediate ($1.4 \pm 0.02\%$) to organic soil sites ($2.0 \pm 0.04\%$) (Table 1).

Regionally, lowest TP concentrations were opposite those of OC and TN. The highest concentrations occurred at the river mouths (0.38, 0.50, and 0.47 mg cm^{-3} at sites WSC-6, 10, and 13, respectively), and lowest concentrations occurred at sites WSC-1, 2, and 3 furthest up the Shark River (0.08 , 0.06 , and 0.07 mg cm^{-3} , respectively). When compared by soil class, TP% decreased significantly from mineral (0.44 ± 0.013) to intermediate (0.18 ± 0.003) to organic soil sites ($0.08 \pm 0.003 \text{ mg cm}^{-3}$) (Table 1).

In terms of nutrient ratios, OC/TN of site classes was greater in the downstream mineral sites (32.2 ± 1.39) compared to the organic and intermediate sites, and site-specific TN/TP increased significantly with distance from the GOM ($r = 0.93$, $P < 0.01$) (Table 2). This indicates that limitation of TP within the region is most pronounced furthest from its marine source. The lowest mean OC/TN ratios occurred at the mouth of the Shark River (WSC-6: 19.0 ± 0.82) and the highest ratio was found at site WSC-13 on the Broad River (47.6 ± 2.60). There was no statistically significant difference between OC/TN at the organic (23.7 ± 0.53) and intermediate (22.7 ± 0.41) sites ($P > 0.05$); however, the mineral sites (32.2 ± 1.39) were significantly greater ($P < 0.05$; Table 1) than the other two soil classes. The highest TN/TP occurred in the upper Shark River (WSC-1: 96.0 ± 3.5) and the lowest at the mouth of the Harney (WSC-10: 10.2 ± 0.4) (Table 1). Ratios increased significantly ($P < 0.05$) from mineral (12.9 ± 0.6) to intermediate (34.4 ± 1.3) to organic (81.3 ± 3.2) site classes. Similarly, TN/TP was negatively correlated with total mass of soil deposition across sites ($r = -0.71$, $P < 0.01$), indicating that the locations of greatest mass deposition and TP availability are closest to the coast.

100-Year Burial Rates of OC, CaCO_3 , TN and TP

Overall, there was relatively little variability in 100-year OC burial rates, with a regional mean of $133.8 \pm 12.0 \text{ g OC m}^{-2} \text{ y}^{-1}$ (Table 3). In contrast to soil OC concentrations (Table 1), there was no consistent pattern in OC burial rates as a function of distance from the GOM. Of the two sites with the lowest OC burial rates, one was 69 (WSC-2, 18 km upstream) and the other was 83 (WSC-3, 13 km upstream) $\text{g OC m}^{-2} \text{ y}^{-1}$ (Table 3). The two sites with the highest burial rates were at the mouth of the Harney and Broad Rivers (WSC-10: 212, and WSC-13: $204 \text{ g OC m}^{-2} \text{ y}^{-1}$). There was no significant difference in OC burial rates between site classes ($P > 0.05$) (Figure 3C). However, a modified Thompson Tau test indicated that the OC burial rate for site WSC-1 was an outlier with a higher 100-year burial rate than the other three upstream organic sites. Therefore, if that site is excluded from the comparison, the mean of the remaining three organic sites (79.0 ± 5.3) was significantly lower than the intermediate sites (144.1 ± 6.3) ($P < 0.05$) but was not different from the mineral sites (161.8 ± 27.2) ($P > 0.05$). Burial rates of OC were positively correlated with

the soil total mass flux, as well as with burial rates of CaCO_3 and TP, but were negatively correlated with TN/TP (Table 2).

Rates of CaCO_3 burial showed substantial variability, with the highest rates found near the GOM (Tables 2, 3). The regional 100-year mean was $277.2 \pm 114.2 \text{ g m}^{-2} \text{ y}^{-1}$ (Table 3) and ranged from 13 (WSC-2) to 1233 (WSC-13) $\text{g m}^{-2} \text{ y}^{-1}$. As with concentration of CaCO_3 , the 100-year average burial rates increased significantly ($P < 0.05$) from organic (24.9 ± 4.6) to intermediate (121.3 ± 31.7) to mineral sites ($639.4 \pm 233.6 \text{ g m}^{-2} \text{ y}^{-1}$) (Figure 3D). Burial rates of CaCO_3 were also positively correlated with burial rates of OC and TP, and with OC/TN and TN/TP.

The 100-year rates of TN burial varied substantially between cores, ranging from 3.5 (WSC-2) to $8.7 \text{ g m}^{-2} \text{ y}^{-1}$ (WSC-9) (Table 2). There was no significant correlation between TN burial rates and site distance from the GOM ($P > 0.05$; Table 2) nor was there a significant difference of average TN burial rates between the three soil classes ($P > 0.05$) (Figure 3A). In contrast, 100-year TP burial rates were negatively correlated with distance from the GOM ($r = -0.769$; $P < 0.01$; Table 2), increasing from 0.15 ± 0.03 in the upstream organic sites, to 0.51 ± 0.05 in the midstream intermediate sites, and $1.09 \pm 0.18 \text{ g m}^{-2} \text{ y}^{-1}$ in the downstream mineral sites (Figure 3B).

DISCUSSION

Spatial Variability of Soil Accumulation Rates

The GOM is the dominant regional driver of variability in accumulation rates of soil mass, CaCO_3 and TP. Much of this influence is due to storm surge that deposits GOM sediment throughout the coastal Everglades (Whelan and others 2009; Castañeda-Moya and others 2010; Smith and others 2009; Smoak and others 2013). High deposition rates of marine mud at the coast also have a positive influence on soil accretion rates (Breithaupt and others 2017) and the high fluxes of TP are important for supporting mangrove productivity (Chen and Twilley 1999a, b; Childers and others 2006). In contrast to our first hypothesis, the GOM was not a significant predictor of OC burial rates across the region. This is puzzling because OC burial rates are a function of soil OC% and DBD, both of which are influenced by the GOM. Possible explanations for this discrepancy include regional variability in factors including allochthonous OC

Table 2. Pearson Correlation (*r*) Matrix for Site Variables Including Distance (km) from the Gulf of Mexico, 100-Year Mean Soil Fluxes ($\text{g m}^{-2} \text{y}^{-1}$), Nutrient Ratios, and Forest Stand Characteristics

	Distance	Soil mass flux	TOC flux	CaCO ₃ flux	TN flux	TP flux	OC/TN	TN/TP	Stem density	Aboveground biomass	Complexity index	Basal area
Distance	–											
Soil mass flux	–.663*	–										
TOC flux	–.513	.842**	–									
CaCO ₃ flux	–.597*	.980**	.784**	–								
TN flux	–.343	0.256	.609*	0.104	–							
TP flux	–.769**	.935**	.783**	.854**	0.419	–						
OC/TN	–.327	.789**	N/A	.877**	–.176	0.533	–					
TN/TP	.933**	–.710**	–.619*	–.616*	–.477	N/A	–.317	–				
Stem density	.724*	–.486	–.456	–.447	–.423	–.55	–.236	0.652	–			
Aboveground biomass	–.215	–.101	–.137	–.127	0.181	–.051	–.181	–.197	0.02	–		
Complexity index	0.311	–.32	–.163	–.343	–.01	–.317	–.207	0.215	N/A	0.426	–	
Basal area	–.447	0.047	0.042	–.004	0.338	0.111	–.103	–.349	–.151	N/A	0.256	–

Significant values are indicated by * ($P < 0.05$) and ** ($P < 0.01$). N/A indicates not applicable because of dependency between variables.

deposition, belowground productivity, and rates of soil respiration.

Compared to global variability of OC burial rates in mangrove environments that range from 10 to greater than $1000 \text{ g m}^{-2} \text{y}^{-1}$ (Breithaupt and others 2012), OC burial rates in the southwestern Everglades exhibit only moderate spatial variability with a range of $69\text{--}212 \text{ g m}^{-2} \text{y}^{-1}$ (Table 3). Greater variability might be found if basin sites (Lugo and Snedaker 1974) had been sampled. The minimal fluxes of allochthonous sediment in interior basin sites would likely contribute to lower rates than those seen along the river margins, a hypothesis supported by the positive correlation between soil mass flux and OC burial across the region (Table 2).

The three upstream sites located near Tarpon Bay (Figure 1b; WSC-2, 3, and 7), were the most nutrient limited (TN/TP 57–86; Table 1) and had rates of OC burial lower than at any other sites in this study (Table 3). One hypothesis for the low rates at these sites is that sea level rise has introduced pulses of seawater sulfate into historically freshwater soils, which has led to enhanced soil OC oxidation (Chambers and others 2015). This hypothesis is supported by data showing a 5–15 salinity increase in the annual maximum groundwater salinity in the past decade at site WSC-2 (Saha and others, 2012). Site WSC-1, which is about 7 km upstream of Tarpon Bay, may represent a freshwater end-member that has yet to experience elevated seawater salinity. Surface water salinity at this site was 0.67 at the time of core collection in the regional dry season at high tide. If this SLR hypothesis for the low OC burial rates in the region around Tarpon Bay is correct, then the oligohaline region of the Everglades appears to be a vulnerable source of OC where historically preserved soil carbon may be oxidized back to the atmosphere or exported as particulate and/or dissolved organic and inorganic carbon. Another possible driver of the low rates near Tarpon Bay could be erosion and translocation of the soil during high freshwater events or generally poorer efficiency for retaining soil carbon.

Nutrient limitation, specifically high TN/TP, leads mangrove to increase root production in order to acquire belowground resources (Castañeda-Moya and others 2013). Therefore, it might be expected that OC burial rates (which include root OC) would be negatively correlated with TP burial rates and positively correlated with TN/TP. Instead, these data show the opposite, with a positive correlation to TP burial rates ($r = 0.78$, $P < 0.01$) and a negative correlation with TN/TP ($r = -0.62$;

Table 3. 100-Year Mean (± 1 SE) Accumulation Rates of Organic Carbon, Total Nitrogen, Total Phosphorous, Calcium Carbonate, and Total Soil Mass by Site

River	Site classification	Site	Accumulation rate ($\text{g m}^{-2} \text{yr}^{-1}$)				
			TOC	CaCO_3	TN	TP	Total mass
Shark	Organic	WSC-1	135 (8.6)	27 (1.7)	7.1 (0.5)	0.18 (0.01)	320 (20.4)
	Organic	WSC-2	69 (5.8)	13 (1.1)	3.5 (0.3)	0.10 (0.01)	164 (13.8)
	Organic	WSC-3	83 (4.9)	25 (1.3)	3.8 (0.2)	0.11 (0.01)	217 (12.6)
	Intermediate	WSC-4	157 (13.0)	119 (9.0)	7.2 (0.7)	0.48 (0.04)	540 (45.4)
	Intermediate	WSC-5*	123 (7.8)	N/A	7.0 (0.6)	0.56 (0.03)	568 (61.2)
	Mineral	WSC-6	104 (13.3)	251 (30.7)	6.2 (0.8)	0.79 (0.10)	724 (91.1)
Harney	Organic	WSC-7	86 (12.6)	35 (5.2)	4.5 (0.6)	0.21 (0.03)	233 (34.1)
	Intermediate	WSC-8	137 (9.1)	86 (5.6)	6.8 (0.4)	0.44 (0.03)	465 (30.8)
	Intermediate	WSC-9	152 (12.4)	221 (15.8)	8.7 (0.7)	0.69 (0.05)	729 (57.6)
	Mineral	WSC-10	212 (23.7)	1039 (111.6)	7.2 (0.8)	1.59 (0.21)	2054 (238.9)
Broad	Intermediate	WSC-11	153 (11.2)	59 (4.3)	7.1 (0.5)	0.40 (0.03)	463 (35.3)
	Mineral	WSC-12	127 (21.4)	219 (29.9)	6.5 (1.2)	0.87 (0.16)	822 (136.5)
	Mineral	WSC-13	204 (38.2)	1233 (239.2)	5.4 (0.9)	1.10 (0.21)	1988 (385.4)
	All sites		133.8 (12.0)	277.2 (114.2)	6.2 (0.4)	0.58 (0.12)	714.3 (170.6)

Flux uncertainties for individual sites represent the respective proportions of the total sediment mass accumulation error calculated following Binford (1990).

*WSC-5 data are from Breithaupt and others (2014).

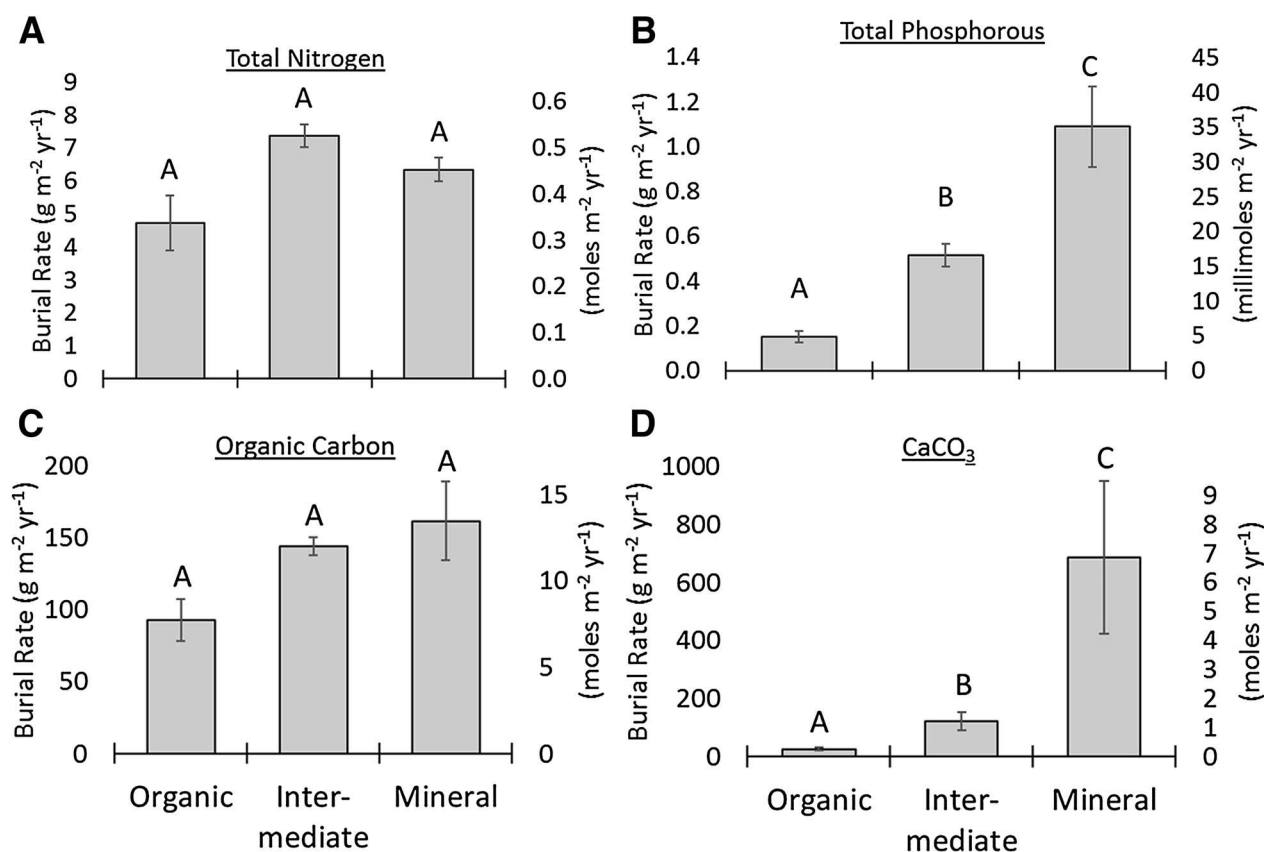


Figure 3. Mean (± 1 SE) burial rates by site classification. Different capital letters above error bars indicate significant difference ($P < 0.05$). Rates are provided in mass units on the primary axis, and molar units on the secondary axis.

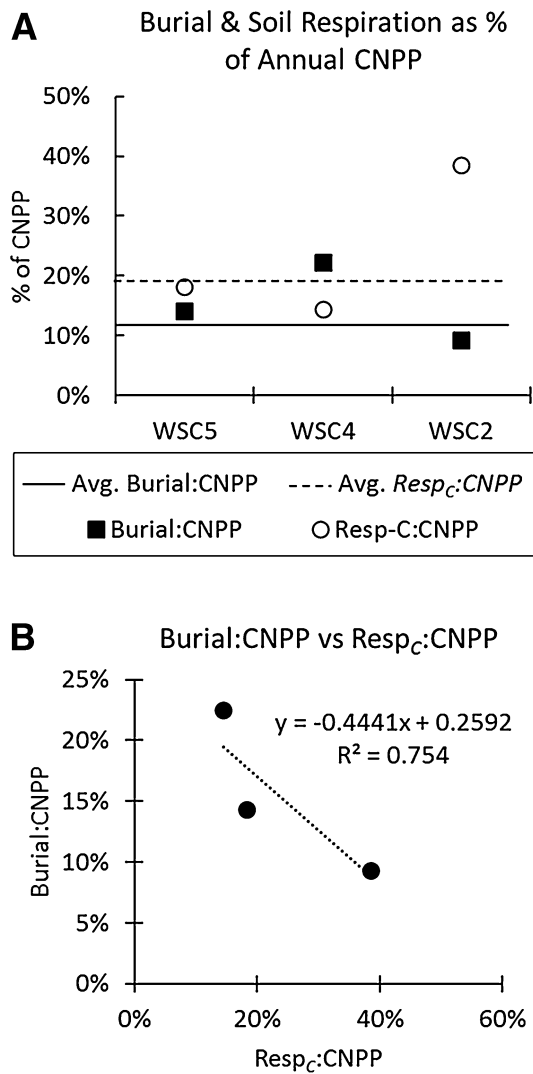


Figure 4. **A** Organic carbon burial (black squares) and soil C respiration (open circles; Troxler and others 2015) as a percentage of site-specific mangrove carbon net primary productivity (CNPP) (Castañeda-Moya and others 2013) for sites that are 4, 8, and 18 km upstream from the GOM. Solid line (12.1%) represents global average burial/CNPP (Breithaupt and others 2012). Dashed line (19.3%) represents global average Resp_C/CNPP (Bouillon and others 2008). **B** Comparison of burial efficiency (Burial/CNPP) and soil respiration as a fraction of NPP (Resp_C/CNPP).

$P < 0.05$) (Table 2). These observations indicate that root productivity is not the sole driver of soil OC inputs across the estuary. In addition to production and delivery of allochthonous material, other influences on OC burial rates include biogeochemical conditions related to the preservation of soil carbon including water level and inundation time (Dessu and others 2018) and changing salinity (Chambers and others 2013) among others.

Organic Carbon Burial Efficiency and Soil Respiration

The efficiency of OC burial at these sites was determined by normalizing 100-year rates to CNPP (Figure 4A, black squares), and is interpreted as the percentage of annual OC production expected to remain buried in the soil over 100 years. This comparison assumes constant CNPP in the past century, which may be unlikely given the effect of disturbance events and regional observations of a 5% reduction in ecosystem CO₂ uptake following substantial (that is, +10 ppt) increases in salinity (Barr and others 2012). However, the comparison serves as a good first-order estimate as global mangrove carbon budgets also rely on this assumption when deriving a global average OC Burial/CNPP of 12.1 (Bouillon and others 2008; Alongi 2009). The upstream site (WSC-2) was the least efficient at burying OC (9%) and was slightly less than the global estimate, whereas WSC-5 was slightly higher (14%) and WSC-4 was nearly twice as efficient (22%).

Similarly, a pattern in the spatial variability of OC burial efficiency is also discernible by comparisons with soil respiration (Figure 4A open circles). The global average for soil respiration/CNPP is 19.3% (Bouillon and others 2008). At site WSC-2, where burial was the least efficient, the soil respiration as a fraction of NPP was highest (39%), nearly twice that of the global estimate. At site WSC-4 where burial has been most efficient, soil respiration was lowest (14%); site WSC-5 was 18%. A comparison of the two ratios indicates a strong anti-correlation, where OC burial efficiency declines as soil respiration increases (Figure 4B). There is a timescale uncertainty associated with these comparisons, as soil respiration represents a series of five measurements over 4 years, and it is unlikely that these values are representative of the past century. However, this evidence from different methods presents an indication of spatially variable belowground processes occurring in the coastal Everglades.

Relationship Between Soil Accumulation Rates and Aboveground Vegetation Characteristics

Contrary to our first hypothesis, there was no correlation between soil accumulation rates, including nutrient fluxes, and aboveground vegetation characteristics (Table 2). The aboveground characteristics we measured may exhibit periodic declines caused by disturbances such as storms,

fires, and freezes (Smith and others 1994; Barr and others 2012; Danielson and others 2017) whereas soil accumulation rates are less susceptible to loss from these types of disturbance (barring erosion) and often demonstrate increased sedimentation (Smith and others 2009; Smoak and others 2013). Because many of our vegetation measurements were made after hurricane Wilma (2005) damaged many of these sites (Smith and others 2009), it is possible that the lack of substantial differences in vegetation characteristics can be attributed to different stages of recovery within the region (Danielson and others 2017). Another possible reason for the lack of correlation between soil accumulation rates and aboveground vegetation characteristics is that the spatial variability of aboveground biomass at these coring locations was less than might be found if sites were included further from the main tidal creeks as well as further upstream in the northern rivers (Plates 2 and 3 from Simard and others 2006). The range in biomass at these sites was 67 Mg ha^{-1} (Figure 2A), which is much smaller than the range of 200 Mg ha^{-1} identified by Simard and others (2006) for the region as a whole.

Castañeda-Moya and others (2013) found that soil TP density (mg cm^{-3}) over the 0–50 cm depth interval explains 52% of variability in mangrove aboveground biomass across sites in Florida, Mexico and Micronesia. Their model weakly explains seven of our sites, with a regression standard error of 23.27 Mg ha^{-1} (Figure 5). However two of our sites (WSC-10 and 13 at the mouths of the Harney and Broad Rivers) had soil TP densities over twice that of the other sites, but the aboveground biomass was 106 and 118 Mg ha^{-1} less than the model of Castañeda-Moya and others (2013) predicts. This may indicate that the fraction of TP available for utilization by mangroves is lower at these sites where CaCO_3 concentrations are highest in the region (Table 1). Another possibility is biomass at these sites closest to the coast was lower than expected because of damage following hurricane Wilma in 2005.

Regional Carbon Budget Implications

Spatial variability of both OC and CaCO_3 have important implications for the regional carbon budget (Troxler and others 2013). These findings provide strong evidence of numerous regional differences in multiple pools of the mangrove carbon budget: production, burial, soil respiration, and potentially (by mass balance) aqueous export. Our estimate is that approximately 10–20% of organic

carbon is buried for a century or more at these sites. The values from Troxler and others (2015) suggest that, regionally, 14–38% of fixed carbon is lost to the atmosphere via soil respiration. Troxler and others (2013) estimated an aqueous flux of carbon (dissolved and particulate OC, and dissolved inorganic carbon) as $131 \pm 155 \text{ g m}^{-2} \text{ y}^{-1}$, which equates to 15–41% of the annual production at these sites (Castañeda-Moya and others 2013). These terms (burial, soil respiration, and aqueous fluxes) sum to 39–99% of production.

The efflux of pore water dissolved inorganic carbon (DIC) is an important component of the global mangrove carbon budget (Alongi 2014; Bouillon and others 2008; Maher and others 2013) and can contribute substantial DIC/alkalinity to the nearshore environment (Maher and others 2013; Sippo and others 2016). In the coastal Everglades non-respiration sources of DIC may potentially include dissolution of carbonate mud within the mangroves and underlying limestone bedrock. From December 2000 to February 2018 the pH average ($\pm 1 \text{ SD}$) of the surface water within the forest was 6.73 ± 0.77 at site WSC-2, 6.91 ± 0.96 at site WSC-4, and 7.12 ± 0.92 at site WSC-5 (Castañeda and Rivera-Monroy 2018). These data suggest that at times mangrove peat may be an unstable environment for carbonate. Acidic conditions may be produced by root excretions and decaying organic matter (Egler 1952) and include carbonic acid formed by aerobic respiration, nitric acid formed by nitrification, and sulfuric acid following oxidation of sulfides and iron sulfides (Aller 1982; Walter and Burton 1990; Middelburg and others 1996). Observations of carbonate loss have

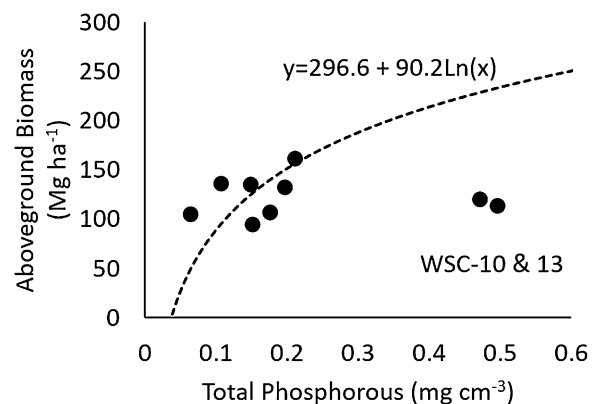


Figure 5. Aboveground biomass (y) as a function of soil total phosphorous (x) (black circles) compared with model from Castañeda-Moya and others (2013) (dashed line). The standard error of the regression (S) was 23.27 Mg ha^{-1} . Outlier sites WSC-10 & 13 are noted in the dashed square.

been reported in mangroves of the Herbert River estuary in north Queensland, Australia (Brunskill and others 2002). This suggests that DIC measurements in these environments (Ho and others 2017) may include both respiration and dissolution products, and partitioning the relative contributions of each should be considered in future research to constrain the regional carbon budget.

CONCLUSIONS

Efforts to constrain local carbon budgets are being undertaken in numerous coastal environments around the world because of great variability in the rates of production, export, and sequestration, and the need to provide greater precision in global carbon models (Bauer and others 2013). Although the southwest Everglades represent one of the most well-studied mangrove carbon budgets in the world, with numerous studies focused on the overall budget as well as its individual components that date back over 20 years, there are still many questions and large uncertainties in the mass balance (Troxler and others 2013 and references therein). This research quantified soil burial rates across a landscape gradient that exhibits substantial aboveground biomass variability reflective of the P-limitation in the estuary. Both OC and TN showed little variability across sites, with 100-year burial rates of $144 (\pm 12)$ and $6 (\pm 0.4) \text{ g m}^{-2} \text{ y}^{-1}$, respectively. Conversely, TP and CaCO_3 burial rates averaged $0.58 (\pm 0.12)$ and $277 (\pm 114) \text{ g m}^{-2} \text{ y}^{-1}$, respectively, with the highest values found nearest the coast in locations that are most frequently influenced by marine frontal systems and storms. Although OC burial rates showed no clear relationship with standing aboveground vegetation characteristics, substantial differences between sites were identified when considered in the context of NPP and soil respiration. The greatest burial efficiency occurred in the mid-estuary, intermediate soil sites with 22% of fixed C being sequestered for a century. Organic C burial was least efficient near Tarpon Bay; increasing salinity (with the potential for sulfate reduction) has been observed in this oligohaline part of the ecotone in the past decade. These findings suggest that accelerating SLR may cause the loss of historically sequestered carbon even in the absence of catastrophic peat collapse. The finding of a negative correlation between OC burial and soil respiration suggests a profitable venue for future research to further understand the inputs and efficiency of preservation for soil carbon across the region.

ACKNOWLEDGEMENTS

The authors thank the following individuals for field and laboratory assistance: Kailey Comparetto, Amanda Chappel, Jessica Jacobs, Ding He, Lindsay Brendis, Mason Jeffers, Jared Ritch. This work was funded by the University of South Florida College of Marine Science fellowships provided by Anne and Werner Von Rosenstiel and the St. Petersburg Downtown Partnership; the US Environmental Protection Agency STAR Fellowship [Grant No. F13B20216] and the National Science Foundation South Florida Water, Sustainability and Climate program [Grant No. EAR-1204079] to JMS. CJS was supported by the Australian Research Council (DE160100443 and DP150103286). Data sets were provided by the Florida Coastal Everglades Long-Term Ecological Research (LTER) Program, supported by the National Science Foundation under Grant Nos. DEB-1237517, DBI-0620409, and DEB-9910514.

REFERENCES

- Abohassan A, Tewfik SFA, Wakeel AOE. 2010. Effect of thinning on the above ground biomass of (*Conocarpus erectus* L.) trees in the western region of Saudi Arabia. *J King Abdulaziz Univ Meteorol Environ* 21:3–17.
- Aller RC. 1982. Carbonate dissolution in nearshore terrigenous muds: the role of physical and biological reworking. *J Geol* 90:79–95.
- Alongi D. 2009. The energetics of mangrove forests. Berlin: Springer.
- Alongi D, Pfitzner J, Trott L, Tirendi F. 2005. Rapid sediment accumulation and microbial mineralization in forests of the mangrove *Kandelia candel* in the Jiulongjiang Estuary, China. *Estuarine, Coastal ...* 63:605–18.
- Alongi D, Trott L, Wattayakorn G, Clough B. 2002. Below-ground nitrogen cycling in relation to net canopy production in mangrove forests of southern Thailand. *Mar Biol* 140:855–64.
- Alongi DM. 2014. Carbon cycling and storage in mangrove forests. *Ann Rev Mar Sci* 6:195–219.
- Alongi DM, Sasekumar A, Chong VC, Pfitzner J, Trott LA, Tirendi F, Dixon P, Brunskill GJ. 2004. Sediment accumulation and organic material flux in a managed mangrove ecosystem: estimates of land–ocean–atmosphere exchange in peninsular Malaysia. *Mar Geol* 208:383–402.
- Amundson R. 2001. The carbon budget in soils. *Annu Rev Earth Planet Sci* 29:535–62.
- Anderson GH, Smith TJ III, Balentine KM. 2014. Land-margin ecosystem hydrologic data for the coastal Everglades, Florida, water years 1996–2012: U.S. Geological Survey Data Series 853, 38 p., <https://dx.doi.org/10.3133/ds853>.
- Appleby PG. 2001. Chronostratigraphic techniques in recent sediments. In: Smol JP, Birks HJB, Last WM, Eds., *Tracking environmental change using lake sediments*. Kluwer Academic Publishers, New York. Vol 1, Ch 9
- Barr JG, Engel V, Fuentes JD, Fuller DO, Kwon H. 2012. Satellite-based estimates of light-use efficiency in a subtropical

- mangrove forest equipped with CO₂ eddy covariance. *Bio-geosciences Discuss* 9:16457–92.
- Bauer JE, Cai W-J, Raymond PA, Bianchi TS, Hopkinson CS, Regnier PAG. 2013. The changing carbon cycle of the coastal ocean. *Nature* 504:61–70.
- Binford MW. 1990. Calculation and uncertainty analysis of 210Pb dates for PIRLA project lake sediment cores. *J Paleolimnol* 3:253–67.
- Boto KG, Wellington JT. 1984. Soil Characteristics and Nutrient Status in a Northern Australian Mangrove Forest. *Estuaries* 7:61–9.
- Bouillon S, Borges AV, Castañeda-Moya E, Diele K, Dittmar T, Duke NC, Kristensen E, Lee SY, Marchand C, Middelburg JJ, Rivera-Monroy VH, Smith TJ, Twilley RR. 2008. Mangrove production and carbon sinks: a revision of global budget estimates. *Global Biogeochem Cycles* 22:1–12.
- Boyer JN. 2006. Shifting N and P limitation along a north-south gradient of mangrove estuaries in South Florida. *Hydrobiologia* 569:167–77.
- Breithaupt JL, Smoak JM, Rivera-Monroy VH, Castañeda-Moya E, Moyer RP, Simard M, Sanders CJ. 2017. Partitioning the relative contributions of organic matter and mineral sediment to accretion rates in carbonate platform mangrove soils. *Mar Geol* 390:170–80.
- Breithaupt JL, Smoak JM, Smith TJ, Sanders CJ. 2014. Temporal variability of carbon and nutrient burial, sediment accretion, and mass accumulation over the past century in a carbonate platform mangrove forest of the Florida Everglades. *J Geophys Res Biogeosciences* 119:2032–48.
- Breithaupt JL, Smoak JM, Smith TJ, Sanders CJ, Hoare A. 2012. Organic carbon burial rates in mangrove sediments: strengthening the global budget. *Global Biogeochem Cycles* 26:1–11.
- Brunskill GJ, Zagorski I, Pfitzner J. 2002. Carbon burial rates in sediments and a carbon mass balance for the Herbert River region of the Great Barrier Reef continental shelf, north Queensland, Australia. *Estuar Coast Shelf Sci* 54:677–700.
- Castaneda E, Rivera-Monroy V. 2018. Abiotic monitoring of physical characteristics in porewaters and surface waters of mangrove forests from the Shark River Slough and Taylor Slough, Everglades National Park (FCE), South Florida from December 2000 to Present. Environmental Data Initiative. <http://dx.doi.org/10.6073/pasta/1f61bffd880b6c90d31d92f501bfe3be>. Dataset accessed March 8, 2018
- Castañeda-Moya E, Twilley RR, Rivera-Monroy VH. 2013. Allocation of biomass and net primary productivity of mangrove forests along environmental gradients in the Florida Coastal Everglades, USA. *For Ecol Manage* 307:226–41.
- Castañeda-Moya E, Twilley RR, Rivera-Monroy VH, Zhang K, Davis SE, Ross M. 2010. Sediment and nutrient deposition associated with hurricane Wilma in mangroves of the Florida coastal everglades. *Estuaries and Coasts* 33:45–58.
- Chambers LG, Davis SE, Troxler TG. 2015. Sea level rise in the everglades: plant-soil-microbial feedbacks in response to changing physical conditions. *Microbiology of the Everglades ecosystem*. Boca Raton: CRC Press. p 89–112.
- Chambers LG, Osborne TZ, Reddy KR. 2013. Effect of salinity-altering pulsing events on soil organic carbon loss along an intertidal wetland gradient: a laboratory experiment. *Biogeochemistry* 115:363–83.
- Chen R, Twilley R. 1999a. Patterns of mangrove forest structure and soil nutrient dynamics along the Shark River estuary, Florida. *Estuaries and Coasts* 22:955–70.
- Chen R, Twilley RR. 1999b. A simulation model of organic matter and nutrient accumulation in mangrove wetland soils. *Biogeochemistry* 44:93–118.
- Childers D, Boyer J, Davis S, Madden C, Rudnick D, Sklar F. 2006. Relating precipitation and water management to nutrient concentrations in the oligotrophic ‘upside-down’ estuaries of the Florida Everglades. *Limnol Oceanogr* 51:602–16.
- Chmura GL, Anisfeld SC, Cahoon DR, Lynch JC. 2003. Global carbon sequestration in tidal, saline wetland soils. *Global Biogeochem Cycles*. <https://doi.org/10.1029/2002GB001917>.
- Danielson TM, Rivera-Monroy VH, Castañeda-Moya E, Briceño H, Travieso R, Marx BD, Gaiser E, Farfán LM. 2017. Assessment of Everglades mangrove forest resilience: implications for above-ground net primary productivity and carbon dynamics. *For Ecol Manage* 404:115–25. <https://doi.org/10.1016/j.foreco.2017.08.009>.
- Davidson EA, Janssens IA. 2006. Temperature sensitivity of soil carbon decomposition and feedbacks to climate change. *Nature* 440:165–73.
- Dean WE. 1974. Determination of carbonate and organic matter in calcareous sediments and sedimentary rocks by loss on ignition: comparison with other methods. *J Sediment Res* 44:242–8.
- De Deyn GB, Cornelissen JHC, Bardgett RD. 2008. Plant functional traits and soil carbon sequestration in contrasting biomes. *Ecol Lett* 11:516–31.
- Dessu SB, Price RM, Troxler TG, Kominoski JS. 2018. Effects of sea-level rise and freshwater management on long-term water levels and water quality in the Florida Coastal Everglades. *J Environ Manage* 211:164–76.
- Donato DC, Kauffman JB, Murdiyarso D, Kurnianto S, Stidham M, Kanninen M. 2011. Mangroves among the most carbon-rich forests in the tropics. *Nat Geosci* 4:293–7.
- Egler FE. 1952. Southeast Saline Everglades Vegetation, Florida, and its management. *Vegetatio* 3:213–65.
- Haigh ID, Wahl T, Rohling EJ, Price RM, Pattiaratchi CB, Calafat FM, Dangendorf S. 2014. Timescales for detecting a significant acceleration in sea level rise. *Nat Commun*. <https://doi.org/10.1038/ncomms4635>.
- Ho DT, Ferrón S, Engel VC, Anderson WT, Swart PK, Price RM, Leticia Barbero L. 2017. Dissolved carbon biogeochemistry and export in mangrove-dominated rivers of the Florida Everglades. *Biogeochemistry* 14(9):2543–59. <https://doi.org/10.5194/bg-14-1-2017>.
- Holdridge LR, Grenke WC, Hatheway WH, Liang T, Tosi JA Jr. 1971. *Forest environments in tropical life zones: a pilot study*. New York: Pergamon Press Inc.
- Jerath M, Bhat M, Rivera-monroy VH, Castañeda-moya E, Simard M, Twilley RR. 2016. The role of economic, policy, and ecological factors in estimating the value of carbon stocks in Everglades mangrove forests, South Florida, USA. *Environ Sci Policy* 66:160–9.
- Lang’at JKS, Kirui BKY, Skov MW, Kairo JG, Mencuccini M, Huxham M. 2013. Species mixing boosts root yield in mangrove trees. *Oecologia* 172:271–8. <https://doi.org/10.1007/s00442-012-2490-x>.
- Levesque VA. 2004. Water flow and nutrient flux from five estuarine rivers along the southwest coast of the Everglades

- National Park, Florida, 1997–2001 (Scientific Investigations Report 2004-5142).
- Lovelock C, Simpson L, Duckett L, Feller I. 2015. Carbon Budgets for Caribbean Mangrove Forests of varying structure and with phosphorus enrichment. *Forests* 6:3528–46.
- Lugo AE, Snedaker SC. 1974. The ecology of mangroves. *Annu Rev Ecol Syst* 5:39–64.
- Maher DT, Santos IR, Gleeson J, Eyre BD. 2013. Groundwater-derived dissolved inorganic and organic carbon exports from a mangrove tidal creek: the missing mangrove carbon sink. *Limnology and Oceanography* 58:475–88.
- Marchio D, Savarese M, Bovard B, Mitsch W. 2016. Carbon sequestration and sedimentation in mangrove swamps influenced by hydrogeomorphic conditions and urbanization in Southwest Florida. *Forests* 7:116.
- Maul GA, Martin DM. 1993. Sea level rise at Key West, Florida, 1846–1992: America's longest instrument record? *Geophys Res Lett* 20:1955–8.
- McLeod E, Chmura GL, Bouillon S, Salm R, Björk M, Duarte CM, Lovelock CE, Schlesinger WH, Silliman BR. 2011. A blueprint for blue carbon: toward an improved understanding of the role of vegetated coastal habitats in sequestering CO₂. *Front Ecol Environ* 9:552–60.
- McVoy C, Said WP, Obeysekera J, VanArman JA, Dreschel TW. 2011. Landscapes and hydrology of the predrainage Everglades. Gainesville: University Press of Florida.
- Middelburg J, Nieuwenhuize J, Slim F, Ohowa B. 1996. Sediment biogeochemistry in an East African mangrove forest (Gazi Bay, Kenya). *Biogeochemistry* 34:133–55.
- Park J, Sweet W. 2015. Accelerated sea level rise and Florida current transport. *Ocean Sci* 11:607–15. <https://doi.org/10.5194/os-11-607-2015>.
- Price RM, Swart PK, Fourqurean JW. 2006. Coastal groundwater discharge—an additional source of phosphorus for the oligotrophic wetlands of the Everglades. *Hydrobiologia* 569:23–36. <https://doi.org/10.1007/s10750-006-0120-5>.
- Rovai AS, Riul P, Twilley RR, Castañeda-Moya E, Rivera-Monroy VH, Williams AA, Simard M, Cifuentes-Jara M, Lewis RR, Crooks S, Horta PA, Schaeffer-Novelli Y, Cintrón G, Pozo-Cajas M, Pagliosa PR. 2016. Scaling mangrove aboveground biomass from site-level to continental-scale. *Glob Ecol Biogeogr* 25:286–98.
- Saha AK, Moses CS, Price RM, Engel V, Smith TJ. 2012. A hydrological budget (2002–2008) for a large subtropical wetland ecosystem indicates marine groundwater discharge accompanies diminished freshwater flow. *Estuaries and Coasts* 35:459–74.
- Sanders CJ, Eyre BD, Santos IR, Machado W, Luiz-silva W, Smoak JM, Breithaupt JL, Ketterer ME, Sanders L, Marotta H, Silva-filho E. 2014. Elevated rates of organic carbon, nitrogen, and phosphorus accumulation in a highly impacted mangrove wetland. *Geophys Res Lett* 41:2475–80.
- Scholl D. 1964. Recent sedimentary record in mangrove swamps and rise in sea level over the southwestern coast of Florida: Part I. *Mar Geol* 1:344–66.
- Simard M, Zhang K, Rivera-Monroy VH, Ross MS, Ruiz PL, Castañeda-Moya E, Twilley RR, Rodriguez E. 2006. Mapping height and biomass of mangrove forests in Everglades National Park with SRTM elevation data. *Photogramm Eng Remote Sens* 72:299–311.
- Sippo JZ, Maher DT, Tait DR, Holloway C, Isaac R. 2016. Are mangroves drivers or buffers of coastal acidification? Insights from alkalinity and dissolved inorganic carbon export estimates across a latitudinal transect. *Global Biogeochem Cycles* 30:753–66.
- Smith TJ, Anderson GH, Balentine K, Tiling G, Ward GA, Whelan KRT. 2009. Cumulative impacts of hurricanes on Florida mangrove ecosystems: Sediment deposition, storm surges and vegetation. *Wetlands* 29:24–34.
- Smith TJ, Hudson H, Robblee MB, Powell GVN, Isdale PJ. 1989. Freshwater flow from the Everglades to Florida Bay: a historical reconstruction based on fluorescent banding in the coral *Solenastrea bournoni*. *Bull Mar Sci* 44:274–82.
- Smith TJ, Robblee MB, Wanless HR, Doyle TW. 1994. Mangroves, hurricanes and lightning strikes. *Bioscience* 44:256–62.
- Smith TJ, Whelan KRT. 2006. Development of allometric relations for three mangrove species in South Florida for use in the Greater Everglades Ecosystem restoration. *Wetl Ecol Manag* 14:409–19.
- Smoak J, Breithaupt J, Smith TJ, Sanders C. 2013. Sediment accretion and organic carbon burial relative to sea-level rise and storm events in two mangrove forests in Everglades National Park. *Catena* 104:58–66.
- Thom BG. 1982. Mangrove ecology: a geomorphological perspective. *Mangrove Ecosystems in Australia*. Canberra: Australian National University Press. pp 3–17.
- Troxler T, Gaiser E, Barr J, Fuentes J. 2013. Integrated carbon budget models for the Everglades terrestrial-coastal-oceanic gradient: current status and needs for inter-site comparisons. *Oceanography* 26:98–107.
- Troxler TG, Barr JG, Fuentes JD, Engel V, Anderson G, Sanchez C, Lagomasino D, Price R, Davis SE. 2015. Component-specific dynamics of riverine mangrove CO₂ efflux in the Florida coastal Everglades. *Agric For Meteorol* 213:273–82. <https://doi.org/10.1016/j.agrformet.2014.12.012>.
- Twilley RR, Rivera-Monroy VH. 2009. Ecogeomorphic models of nutrient biogeochemistry for Mangrove Wetlands. In: Wolanski E, Cahoon DR, Brinson MM, Eds. *Coastal Wetlands: an integrated ecosystem approach*. Amsterdam: Elsevier. p 641–84.
- Twilley RR. 1995. Properties of mangrove ecosystems related to the energy signature of coastal environments. In: Hall CAS, Ed. *Maximum power: the ideas and applications of HT Odum*. Boulder: University of Colorado Press. p 43–62.
- Walter LM, Burton EA. 1990. Dissolution of recent platform carbonate sediments in marine pore fluids. *Am J Sci* 290:601–43.
- Wdowinski S, Bray R, Kirtman BP, Wu Z. 2016. Ocean & Coastal Management Increasing flooding hazard in coastal communities due to rising sea level: case study of Miami Beach, Florida. *Ocean Coast Manag* 126:1–8.
- Whelan KRT, Smith TJ, Cahoon DR, Geological US, International F, Ehan O, Reseat PW, Ave B. 2005. Groundwater control of mangrove surface elevation: shrink and swell varies with soil depth. *Estuaries* 28:833–43.
- Whelan KRT, Smith TJ, Anderson GH, Ouellette ML. 2009. Hurricane Wilma's impact on overall soil elevation and zones within the soil profile in a mangrove forest. *Wetlands* 29:16–23. <https://doi.org/10.1672/08-125.1>.
- Yao Q, Liu K, Platt WJ, Rivera-Monroy VH. 2015. Palynological reconstruction of environmental changes in coastal wetlands of the Florida Everglades since the mid-Holocene. *Quat Res* 83(3):449–58.